

PHASE RELATIONS IN THE SYSTEM Au–Cu–Ag AT LOW TEMPERATURES, BASED ON NATURAL ASSEMBLAGES

JOHN KNIGHT[§]

RR#1, Site 29, Comp. 10, Smithers, British Columbia V0J 2N0, Canada

CRAIG H.B. LEITCH

492 Isabella Point Road, Salt Spring Island, British Columbia V8K 1V4, Canada

ABSTRACT

The composition of some 85 particles of native gold from the 15 Mile rodingite in serpentinite showing in the Coquihalla gold district and the Wheaton Creek placer in the Dease Lake district, British Columbia, falls mainly within the Cu-rich portion of the Au–Ag–Cu phase diagram. The particles display a variety of textures, including exsolution-induced textures. The textures and phase compositions are used to construct a low-temperature phase diagram for the system Au–Ag–Cu. This diagram represents a system that equilibrated for a longer period of time at a lower temperature than is accessible in synthetic systems. In this diagram, the composition AuCu is nearly stoichiometric, a three-phase region is found among AuCu ($\text{Au}_{1.0}\text{Cu}_{0.971}\text{Ag}_{0.003}$), Au_2Cu ($\text{Au}_{2.0}\text{Cu}_{0.962}\text{Ag}_{0.045}$), and $\text{Au}_{3.0}\text{Ag}_{0.71}\text{Cu}_{0.23}$, and there is a two-phase region on the Au side of the Au_2Cu – $\text{Au}_{3.0}\text{Ag}_{0.71}\text{Cu}_{0.23}$ join. There are insufficient data to determine the phase relationships that exist between the compositions Au and Au_2Cu , which includes Au_3Cu . Au_2Cu may or may not be part of a solid solution centered around Au_3Cu . The sequence of formation of extensive exsolution-induced textures and their relation to the other textures seen are explained by combining the phase diagram with a significant shift in the position of the solvi with temperature in this system. Low values of Ag in Au–Cu alloy and of Cu in Au–Ag alloy are reported. Grains of gold alloy from deposits where no Au–Cu alloy is found appear to be undersaturated with respect to Cu.

Keywords: native gold, Au–Ag–Cu alloys, phase diagram, exsolution, composition, 15 Mile showing, Wheaton Creek placer, British Columbia.

SOMMAIRE

La composition d'environ 85 particules d'or natif provenant de l'indice 15 Mile, dans une rodingite associée à une serpentinite du district aurifère de Coquihalla, et du placer de Wheaton Creek, du district de Dease Lake, en Colombie-Britannique, se situe surtout dans la partie riche en cuivre du système Au–Ag–Cu. Ces particules font preuve d'une variété de textures, dont des textures indicatives d'une exsolution. Les textures et la composition des phases servent à construire un diagramme de phases pour le système Au–Ag–Cu approprié à de faibles températures. Ce diagramme représente un système qui a progressé vers un état d'équilibre durant une période de temps beaucoup plus longue que ne serait possible en système synthétique. Dans ce diagramme, la composition AuCu est presque stoechiométrique, une région à trois phases a été découverte impliquant AuCu ($\text{Au}_{1.0}\text{Cu}_{0.971}\text{Ag}_{0.003}$), Au_2Cu ($\text{Au}_{2.0}\text{Cu}_{0.962}\text{Ag}_{0.045}$), et $\text{Au}_{3.0}\text{Ag}_{0.71}\text{Cu}_{0.23}$, et il y a une région à deux phases dans la région vers le pôle Au par rapport à l'assemblage Au_2Cu – $\text{Au}_{3.0}\text{Ag}_{0.71}\text{Cu}_{0.23}$. Les données disponibles ne suffisent pas pour déterminer les relations de phases entre les compositions Au et Au_2Cu , domaine qui inclut Au_3Cu . Le composé Au_2Cu pourrait ou non faire partie d'une solution solide centrée autour de Au_3Cu . La séquence de formation généralisée de textures attribuables à l'exsolution et leurs relations aux autres textures observées peuvent s'expliquer avec ce diagramme de phase, compte tenu du déplacement important du solvus avec la température dans ce système. Nous décrivons de faibles niveaux de Ag dans l'alliage Au–Cu et de Cu dans l'alliage Au–Ag. Les grains d'alliage à dominance d'or provenant des gisements dépourvus d'alliage Au–Cu semblent être sous-saturés par rapport au Cu.

(Traduit par la Rédaction)

Mots-clés: or natif, alliages Au–Ag–Cu, diagramme de phases, exsolution, composition, indice 15 Mile, placer de Wheaton Creek, Colombie-Britannique.

[§] E-mail address: microsci@mail.bulkley.net

INTRODUCTION

Geologists have long recognized that naturally occurring gold is usually an alloy, with Ag being the principal alloying element (Boyle 1979). Naturally occurring Au–Ag alloy commonly contains varying trace amounts of copper, mercury and, more rarely, other elements (*e.g.*, Boyle 1979, Knight & McTaggart 1989). Such Au–Ag alloy is found in all gold deposits containing native gold. In rare instances, the trace elements (*e.g.*, Hg, Cu, Pd, Bi) may occur in sufficient concentration to form an alloy with gold and silver. These compositions of alloy are generally restricted in their occurrence. For example, alloy in the Cu–Au series with >5 wt% Cu are usually only reported from lode deposits associated either with layered mafic intrusions (*e.g.*, Bird *et al.* 1991) or with altered ultramafic rocks (*e.g.*, Murzin *et al.* 1987, Knipe & Fleet 1997) and their associated placers. Knowledge of the phase relations within these alloy compositions can help in the understanding of the formation of their lode hosts. The details of the Au–Cu–Ag and Au–Cu phase diagrams at the lower temperatures of geological interest are not well known because of both the low kinetic rates of separation of the phases in synthetic systems (Okamoto *et al.* 1987) and the rare occurrence of these alloy compositions in nature. It is our aim in this study to use the compositions of naturally occurring Au–Cu–Ag alloy from Wheaton Creek and the 15 Mile showing, in British Columbia, to determine the details of the Au–Cu–Ag phase diagram at low temperatures. The gold at these locations has been equilibrating at near-surface temperature for thousands (if not millions) of years, a condition unavailable in synthetic systems. The data provide a framework for a discussion of the formation of these rare alloy compositions.

PREVIOUS WORK WITHIN THE SYSTEM Au–Cu–Ag

The binary system Au–Ag forms a continuous solid-solution above about 25°C (Dowdell *et al.* 1943, White *et al.* 1957), although Petrovskaya *et al.* (1977) and Petrovskaya & Novgorodova (1980) suggested that Ag-rich alloy may unmix into AuAg and AuAg₃ at low temperatures. The system Au–Cu has been studied both experimentally and theoretically. The experimental studies have been conducted both with and without Ag (Barrett & Massalski 1980, Kogachi & Nakahigashi 1980, Okamoto *et al.* 1987). The properties of synthetic alloy compositions in the Ag-absent system Au–Cu have been reviewed by Knipe & Fleet (1997, Table 1), whereas Okamoto *et al.* (1987) provided a comprehensive review of the experimental results in this system. In the synthetic Ag-absent binary system Au–Cu, a continuous series is found only at temperatures above about 400°C (at 1 atmosphere) (Barrett & Massalski 1980, Okamoto *et al.* 1987). Below 400°C, the phases order into a superlattice structure with miscibility gaps be-

tween them. The resulting Au–Cu phase diagram contains seven phases: Au, Cu, two polymorphs of AuCu (tetra-auricupride), Au₃Cu (auricupride), and two polymorphs of AuCu₃. The phases AuCu and AuCu₃ are well characterized both in synthetic and natural systems (Okamoto *et al.* 1987, Knipe & Fleet 1997), although in synthetic systems their reported compositional range is very large compared to the natural examples. The phase Au₃Cu is not well characterized [*cf.* the findings of Barrett & Massalski (1980) with those of Okamoto *et al.* (1987) and Knipe & Fleet (1997)]. In the Ag-present system Au–Cu, Kogachi & Nakahigashi (1980) used synthetic alloy compositions to create a phase diagram, whereas Kikuchi *et al.* (1980) produced a calculated coherent phase-diagram for the system between 530° and 240°C (Fig. 1). There is a general correspondence between the theoretically expected and synthetic phases, but they differ in detail (Yamauchi *et al.* 1981). The correspondence between the experimental and natural systems is better, but the details predicted in the theoretical study are lacking in the studies of naturally occurring alloy compositions. The theoretical work defined both two- and three-phase regions and documented the general shift of the phase boundaries with temperature. Results of both the theoretical and synthetic studies show a rapid shift of the solvi toward the Au apex as temperature decreases below about 400°C. Below about 200°C, details in the synthetic systems are poorly known; the boundary between the one-phase and two-phase fields near the Au apex is usually drawn as in Figure 2 (curved line nearest Au). The possible multiphase portion around Au₃Cu is usually omitted. These results imply that at low temperatures, Au alloy compositions with both significant Cu and Ag will only be found near the Au apex.

Naturally occurring alloy compositions in the system Au–Cu are rare. Knipe & Fleet (1997) provided a review of many of the reports dealing with natural Au–Cu alloy. The following continues their review. The Urals region is recognized by Russian geologists as a gold-rich metallogenic province in which samples of Au–Ag alloy contain above-average levels of Cu and Hg, and Au–Cu alloy is common (*e.g.*, Murzin & Malyugin 1983, Murzin & Moloshag 1986). Au–Cu alloy (Cu to 2.5 wt%) is associated with chalcopyrite–sphalerite ores in basaltic volcanic rocks (Murzin & Moloshag 1986) and deposits hosted by altered serpentinites (Murzin *et al.* 1987). Novgorodova & Tsepin (1976) described four types of Cu–Au–Ag alloy from the Karabash deposit, Urals. The alloy particles are composites, consisting of a core of AuCu (Ag to 0.55 wt%) with a rim of AuCu₃. An Au–Ag alloy (Ag to 49.3 wt%) with variable levels of mercury (to 10 wt%) also occurs in the core of the particles. A low-Ag alloy with up to 7.5 wt% Cu is found along the contact between AuCu and AuCu₃. Pokrovskii & Berzon (1975) and Pokrovskii *et al.* (1979) reported on the wide variety of alloys in the system Au–Cu–Ag system from the

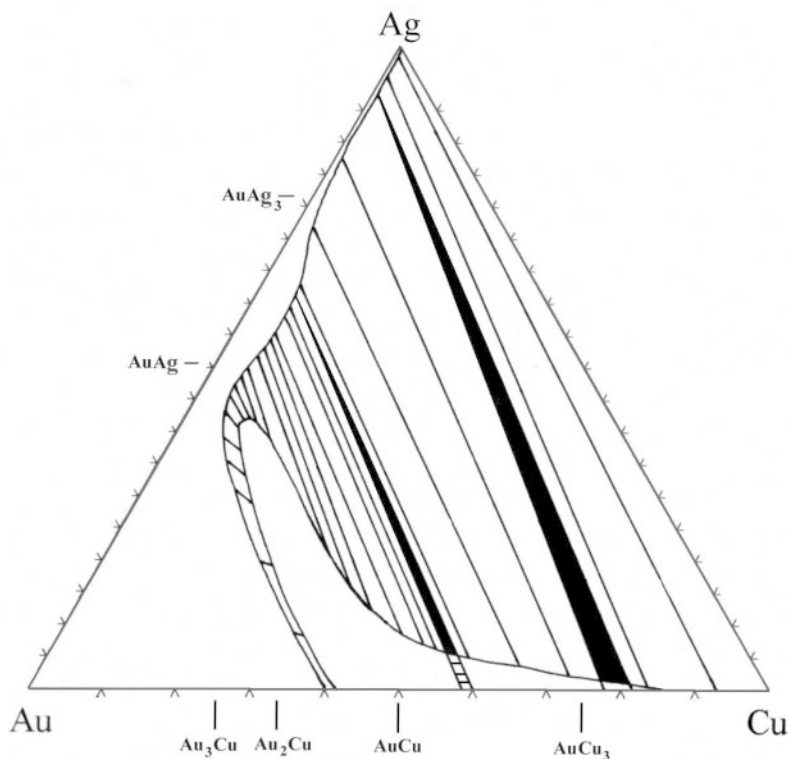


FIG. 1. The calculated phase-diagram for the system Au–Cu–Ag at 240°C, expressed in atomic %, from Kikuchi *et al.* (1980). Black areas denote three-phase assemblages. Tie-lines join phases in two-phase areas.

Zolotaya Gora deposit, southern Urals. The particles of alloy are composites that typically consist of a Cu-poor core and a Cu-rich rim. Figure 1 in Pokrovskii *et al.* (1979) shows the following phases: 1) native copper, 2) native silver, 3) Au–Cu alloy with 40–50 wt% Cu, with up to 1.5 wt% Ag (AuCu_3), 4) 20–30 wt% Cu with up to 2 wt% Ag (AuCu), 5) 0–10 wt% Cu, 2–10% Ag, 6) Au–Ag alloy with 20 wt% Ag, 0–2 wt% Cu, 7) 33–37 wt% Ag, 0 wt% Cu, and 8) 45–55 wt% Ag, 0 wt% Cu, 5–10 wt% Hg (the level of Hg increases with Ag content). By studying etched samples recovered from a “chlorite – garnet – pyroxene” rock (rodingite?) of the southern Urals (Altai–Saiany) and the western slopes of the Urals with an electron microscope, Murzin & Sustavov (1989) were able to describe details of the general exsolution-induced textures in the system Au–Cu–Ag. These textures usually consist of laths of varying thickness, length and taper arranged in subparallel to net-like configurations within the host. They also described the cell parameters of nearly stoichiometric AuCu (both orthorhombic and tetragonal) and AuCu_3 . They reported the occurrence of both orthorhombic and tetragonal AuCu in a single particle of gold. They noted that long-range ordering only occurs in compositions

near stoichiometry. For compositions deviating from stoichiometry, incomplete exsolution results in phases with slight excesses of Au, Cu or Ag with respect to the ideal. They described and illustrated exsolution textures within nearly stoichiometric AuCu and Au_3Cu . For a sample with excess Cu over stoichiometric Au_3Cu , they reported the exsolution of a low-fineness Ag–Au alloy and an Au–Cu alloy. The Au–Cu alloy has the composition 86 wt% Au, 12.0–12.5% Cu, <2.0% Ag, 0% Hg. For a sample with excess Au with respect to Au_3Cu , they reported on the basis of diffraction data that the exsolved Cu-rich phase matches the lines expected of synthetic Au_3Cu . Kuznetsov *et al.* (1977) reported on multiphase Au–Cu alloy compositions ranging from 1 to 31 wt(?)% Cu, 1–15% Ag from heavy-mineral samples within the Donetsk drainage basin, Russia.

Bird *et al.* (1991) reported the presence of Cu–Au and Au–Ag alloys from the Skaergaard layered mafic intrusion, in eastern Greenland. Up to 8 at.% Pd is present in some of the alloys. In terms of the ternary system Au–Cu–Ag, these compositions plot near 47 at.% Au, < 2% Ag, 51% Cu, joining compositions near 70–75 at.%, 5% Cu, 25–30% Ag. From northwestern China, Mao & Liu (1984) reported phases with compo-

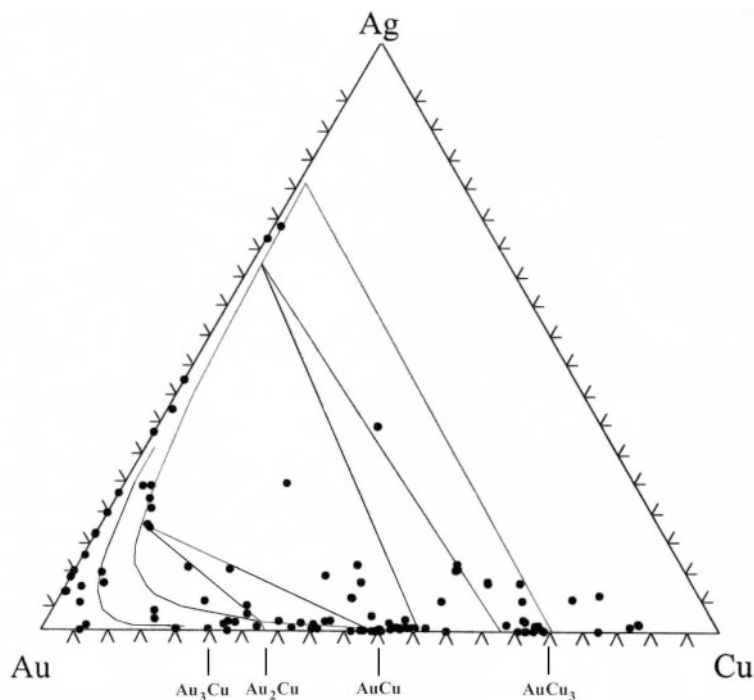


FIG. 2. Data from previous studies of naturally occurring examples of high-Cu gold alloy. The data (in at.%) are taken from the references mentioned in the Previous Work section. For convenience, the phase boundaries presented in Figure 8 also are displayed.

sitions Au_3Cu_2 and Au_2Cu , but were not confident of their results. Bowles (1984) reported Au–Cu alloy compositions in alluvial samples from Sumatra, with compositions 14.5 at.% Au, 79.4% Cu, 6.1% Ag and 52.0 at.% Au, 47.9% Cu and 0.1% Ag in association with Au–Ag alloys of composition 83–100 at.% Au, 17–0% Ag. Stumpfl & Clark (1965, 1966) reported an occurrence in southern Borneo (Kalimantan) of Au–Cu alloy compositions (up to 30 wt% Cu) from alluvial concentrates, associated with platinum-group minerals (PGM). In British Columbia, Raicevic & Cabri (1976) reported an occurrence in alluvial samples of Au–Cu alloy (0–30 wt% Cu, 10–30% Ag) associated with PGM.

Results from these earlier studies are presented in Figure 2 which, for convenience, also displays the phase diagram deduced from this study. The data from the previous studies are presented as reported, with no attempt to separate out compositions referring to multiphase assemblages, or poor-quality analyses. The literature review shows that the phase AuCu is reported most frequently. The phases AuCu₃ and Au₃Cu are reported less frequently than AuCu. From Figure 2, clusters of compositions around AuCu and AuCu₃ are within about 5 at.% of the ideal formula. Compositions do not cluster around Au₃Cu. It is unclear whether at low tem-

peratures this phase is Au₃Cu, part of a solid solution that includes the compositions from Au₂Cu to near Au, or whether the phase Au₃Cu decomposes into a Cu-rich (Au_2Cu ?) and an Au-rich phase. All of these natural phases contain varying amounts of Ag. Some of the other Au–Cu and Au–Cu–Ag alloys that have been reported probably represent mixtures. For example, Mao & Liu (1984) reported on Au₃Cu₂ as a phase, but on the basis of this study and a review of their work, that phase probably represents a mixture of exsolved phases. The description and interpretation of natural Au–Cu phases based on electron-microprobe-derived compositions are complicated by the possibility that exsolved phases may be present but unrecognized because of their very small size (<1 μm).

GEOLOGICAL CONTEXT OF ANALYZED SAMPLES

A literature review reveals that in nearly all cases, Au–Cu alloys are found in ores associated with differentiated mafic magmas, or in serpentinite, rodingite and other altered ultramafic rocks, usually associated with ophiolite complexes. The occurrences of gold sampled for this study are no exception. The 15 Mile lode showing is located in southwestern British Columbia near the

head of 15 Mile Creek, which drains into the Coquihalla River (NTS 92H6 and 92H11) (Ray 1990, Fig. 23, showing #8). The showing lies within a 2-km wide belt of serpentinite, fault-bounded on a regional scale, NW–SE-trending and steeply dipping (Ray 1990). The gold is hosted by rodingites and talc-filled shear zones within the serpentinite body. Cairnes (1930) reported that the thinnest veins of rodingite seem to carry the highest Au grades. He reported that some of the gold is present as smears on talc-lined shear faces, suggesting at least some fault movement after ore formation. There are a number of lode deposits within 4 km of the 15 Mile showing and within 1 km of the fault. They fall into four classes (sulfide-poor quartz or quartz–carbonate veins, sulfide-rich quartz stockworks, talc-lined shear zones, and talc-lined shear zones in rodingite). Although many of the showings have resulted in small mines, the only mine of significance was the Carolin quartz stockwork deposit. Ray (1990) concluded that all the deposits in the area were formed by a “common” mineralizing event that was strongly controlled by the faults bounding the serpentinite body. The fineness [$1000 \times \text{Au wt\%} / (\text{Ag wt\%} + \text{Au wt\%})$] of the gold from all other types of deposit (other than the 15 Mile occurrence) varies from 863 to 907 (Knight & McTaggart 1989, 1990), with a pronounced maximum near a fineness of 870 (78.6 at.% Au and 21.4% Ag). The variation in fineness for a specific lode is small. Cu is present from below detection limit to 0.047 wt% (to 0.12 at.%). Mercury is present in this gold at levels of up to 0.3 wt%, with most values falling between 0.1 and 0.2%. The 15 Mile sample was collected by panning the dump surface and the floor of what was deduced to be the crusher–concentrator. Both are located immediately below the collapsed portal. By comparing the material on the tip and crusher floor, it seems likely that rodingite material was preferentially selected for crushing. The gold sample is considered to represent most of the types of gold mined. Under the microscope, some of the gold in the concentrate could be seen to be intergrown with a pyroxene (diopside?). Magnetite and a garnet also were recognized. Particles in the 0.1 to 0.25 mm range were selected from the concentrate for analysis.

The Wheaton Creek placer is located in north-central British Columbia, at the mouth of Wheaton Creek, where it drains into the Turnagain River (NTS 104I6 and 104I7) (Holland 1940, Fig. 1, Roosevelt Lease). The lode source for the placer gold is unknown, although Holland (1940) concluded that the source was in the immediate vicinity. This is supported by the observation that the gold particles are very weakly deformed, with a low flatness and roundness, with almost no development of a secondary rim (Knight *et al.* 1999). No other lode deposits have been reported from the immediate area. For most of its length, Wheaton Creek drains a 3- to 6-km wide, NW–SE-trending body of serpentinite (Holland 1940). The Wheaton and 15 Mile serpentinite bodies and their bounding faults are part of

a terrane suture joining the Stikinia and Cache Creek terranes (Monger *et al.* 1982). The area was glaciated, and glacial drift covers much of the area. A sample of concentrate, collected in the 1980s from the placer mine, was provided by a miner. Under the microscope, the concentrate is seen to be dominated by magnetite, but numerous particles of native copper, rounded pyrite, minor arsenopyrite, chromian spinel and platinum-group minerals, as well as gold, were also recovered. The native copper is intergrown with bornite in some cases. Holland (1940) reported the presence of much magnetite and a Ni–Fe alloy (awaruite) in the concentrate from mining. He also recovered magnetite, pyrite, pyrrhotite, and chromian spinel from crushed samples of serpentinite. For this study, gold particles in the size range 0.5 to 0.8 mm were selected for analysis.

ANALYTICAL METHODS

In this study, 33 particles of gold alloy from the 15 Mile lode showing and 42 particles of gold alloy from the Wheaton Creek placer were studied by electron-microprobe analysis. The particles were prepared for analysis using the method described in Douma & Knight (1994). A polishing technique that generated the best polish with the minimum cross-contamination was developed by repeated polishing, microscopic observation and analysis of test samples. The polished section for each particle was photographed (examples in Fig. 3) and described under reflected light. The sections were analyzed using a Cameca SX–50 electron microprobe. The analyses were conducted at 20 kV with 100 nA beam current to measure the level of concentration of Cu, Au, Hg, and Ag using $\text{AuM}\alpha$, $\text{AgL}\alpha$, $\text{CuK}\alpha$, and $\text{HgM}\beta$. Pure-element standards were used for Au and Ag; an Au–Cu alloy with 40 wt% Cu and synthetic HgTe were used for Cu and Hg, respectively. The NBS Au–Ag and Au–Cu series of alloy compositions were used as standards. In order to reproduce the compositions of the NBS Au–Cu series of standards, the Au–Cu absorption factor had to be changed. Many of the points selected for analysis using reflected light were checked in the microprobe using back-scattered electron (BSE) imaging. Adjusting the BSE detector for optimal imaging is difficult for small differences at high atomic numbers. As a result, it is probable that not all inhomogeneities were recognized, especially in the Au-rich phases. Hg is present to less than 2 wt%, with all but a few points showing less than 0.5 wt%. The element sums suggest that if other elements are present, values are less than 0.5 wt%. No other elements were recognized in random energy-dispersion X-ray analyses.

Naturally occurring particles of Au–Cu alloy are commonly multiphase (Fig. 4), being composed of either exsolution-induced intergrowths of different Au–Cu alloys (at all scales), or intergrowths of independent phases, or both (Murzin & Sustavov 1989; this study, Fig. 3). Many of the phases approach the minimum size-

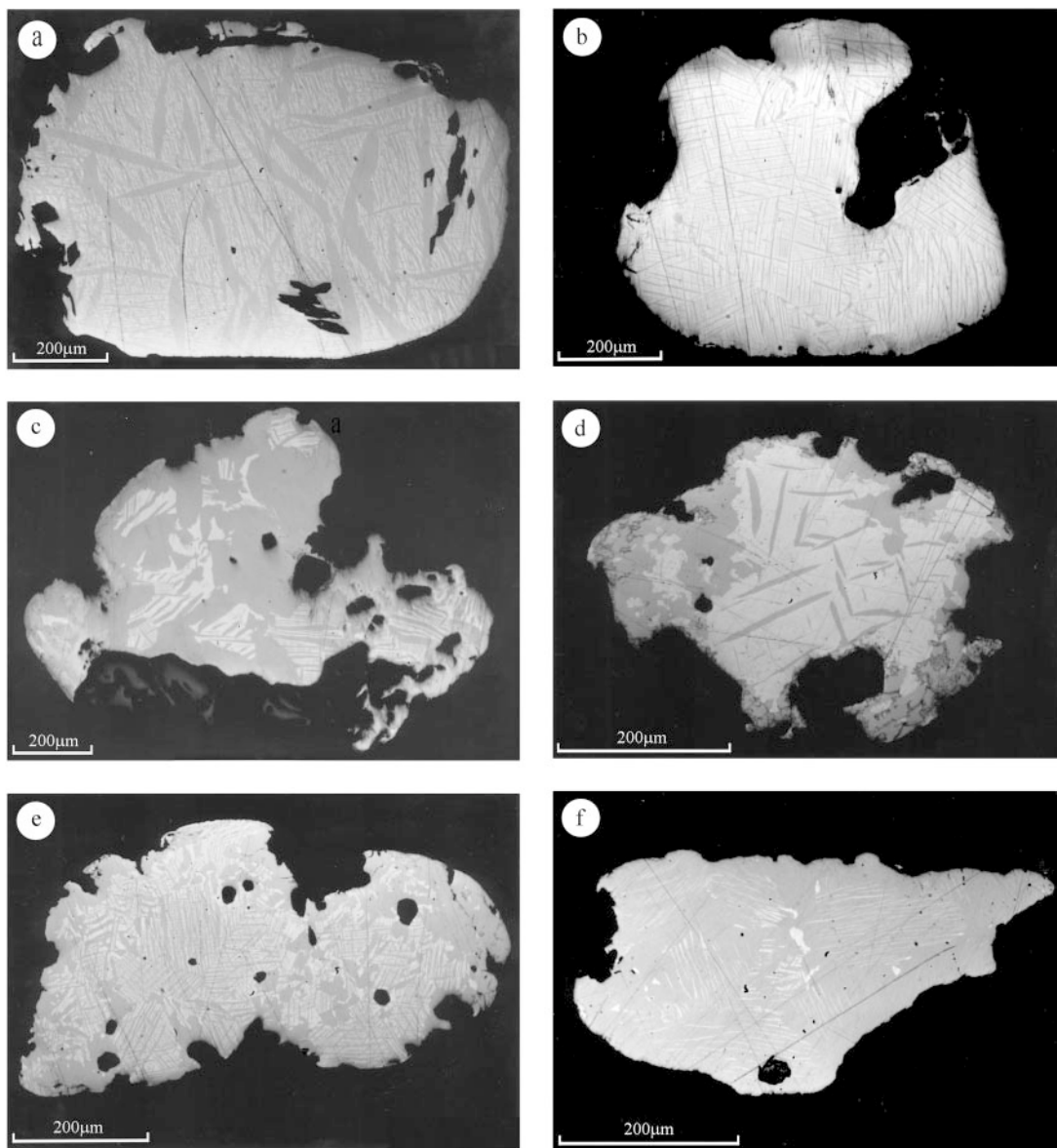


FIG. 3. Reflected-light photographs (uncrossed polars) of polished particles of placer gold from Wheaton Creek. Figures 3a–f illustrate the variation in form and degree of exsolution as well as the range in size and shape of the grains of gold alloy making up the placer particles. Grains are identified by exsolution domains and blebby areas. The blebby texture is illustrated in Figure 3c (dark upper left), and e (dark and light at neck), and the massive texture is shown in Figure 3c (right central margin) and d (lower right margin). Figure 3d illustrates a distinct edge-zone. Light areas are Au-rich, whereas dark areas are Cu-rich. Scale bar is 200 μm for all images.

limit of a few micrometers imposed by electron-microprobe analysis using X rays. Gold alloys are soft, which can result in cross-contamination of the phases during polishing. These two factors impose limits on the inter-

pretation of the analytical data, so that the following tests were conducted to quantify these limits. An idea of the levels of sample-wide contamination through polishing was obtained by measuring the Cu content in

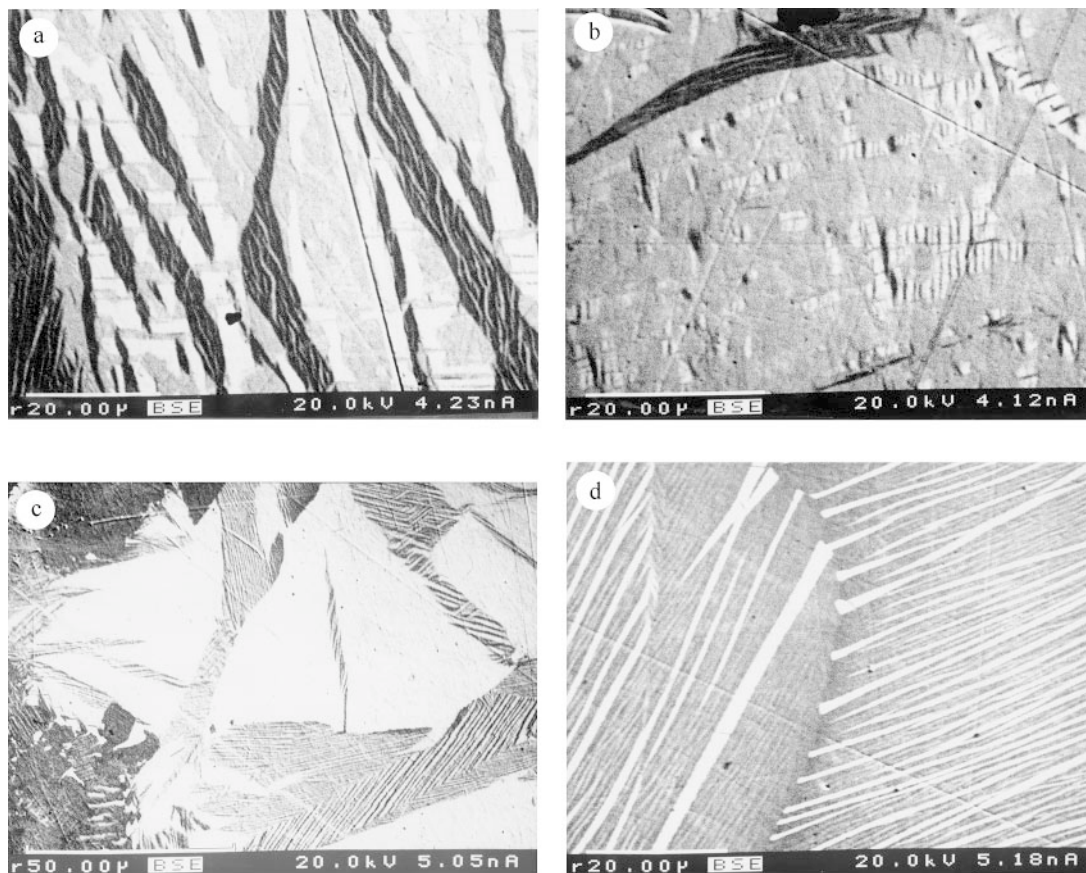


FIG. 4. Details of the exsolution-induced domains as seen in back-scattered electron images. Figures 4a, b and d show material from Wheaton Creek, and Figure 4c shows material from the 15 Mile showing. Figure 4a illustrates details between the dark laths in Figure 3a. The black area at the bottom left of Figure 4a is one of the laths in Figure 3a. The forms seen in Figures 4a and b are interpreted to be the result of exsolution into a developing three-phase region. Figure 4c illustrates blebby phases (bottom left) on the edge of an exsolved area. The presence of extremely small intimately intergrown exsolved domains illustrates one of the difficulties of chemical analysis. These images also illustrate the need for a high-quality polish in order to avoid obscuring details or cross-contaminating the phases by smearing, burnishing, *etc.* Black and grey areas represent Au–Cu alloy with a low level of Ag. Black areas are highest in Cu, grey areas are lowest. White areas are Au–Ag alloy with a low level of Cu.

grains of artificial Cu-free Ag–Au alloy that had been mounted and polished with a particle of pure Cu. Because of the softness of Cu, this test will produce the worst-case contamination. This test revealed that away from the Cu–gold alloy junction, no more than 0.2 wt% Cu was spread across the test sample. To determine the limits of contamination (from preparation) and fluorescence limits (from particle size or nearest neighbor) for analysis within an inhomogeneous particle, a 0.5-mm wire of pure gold was embedded in a 3-mm wire of pure copper, mounted and polished. A line of analysis points was run across the Cu–Au junction. Within the gold, at $>12\ \mu\text{m}$ distance from the Au–Cu junction (equivalent to a particle $>24\ \mu\text{m}$ in diameter), the Cu values in the

gold were between 0.14 and 0.2 wt% Cu (*i.e.*, the level of contamination from sample preparation). The value increased to 0.6 wt% Cu at $6\ \mu\text{m}$ ($12\ \mu\text{m}$ in diameter), 1.0 wt% Cu at $5\ \mu\text{m}$ ($10\ \mu\text{m}$ in diameter), 2.0 wt% Cu at $3\ \mu\text{m}$ ($6\ \mu\text{m}$ in diameter). Because Au–Cu alloys are harder than pure Au or Cu, the contamination values are considered maximum values for this study. On the basis of experience analyzing particles of Au–Ag alloy in brass mounts, we suggest that for relatively small grains of Au–Ag alloy hosted within considerably larger domains of Cu–Au alloy, the maximum contamination of the Au–Ag alloy by copper probably is less than 0.1 wt% Cu, and the total contamination by copper plus fluorescence error is less than 0.5 wt% Cu at a distance

of 10 μm from the contact between the two. It is expected that a contamination error of similar magnitude would arise for small grains of Au–Cu alloy hosted by larger grains of Au–Ag alloy. These results were applied so that exsolution lamellae $<10\ \mu\text{m}$ in diameter were not routinely analyzed, and bulk compositions were obtained for fine exsolution-related mixtures by expanding the spot size to $>10\ \mu\text{m}$ in diameter (+ in Fig. 6, below). Bulk compositions are not used as representatives of phase compositions. Analytical errors common to bulk compositions (*e.g.*, resulting from data-reduction problems) are unlikely to be sufficiently large to affect the conclusions derived from these analytical results.

RESULTS

A review of the data (Table 1, Fig. 5) reveals that the samples from the two geological contexts complement one another, so that the overall interpretation was enhanced by combining the datasets into one. The compositions derived from the 15 Mile sample are lower in Ag content than the particles in the Wheaton sample. For the 15 Mile sample, all but four compositions fall

between AuCu and Au₂Cu. Two of the four fall near 75 at.% Au, with 7 at.% Cu. For the Wheaton Creek sample, about a third of the compositions plot toward the Au–Ag join, with the remainder falling mostly between AuCu and Au₂Cu. This difference in Ag content is reflected in the higher proportion of Wheaton samples that show extensive and complex exsolution-related textures compared to the 15 Mile sample.

The alloy particles were studied in reflected light. Most particles contain gold of more than one composition. Grains of Au–Ag alloy are yellow, whereas grains of Cu-rich Au–Cu alloy are rich pink. The differing compositions outline a variety of textural relationships among grains making up the particle. These textures are well developed in the sample from the Wheaton Creek placer. The textures can be described in terms of three basic types: massive, blebby and exsolved.

Consideration was given to the possibility that the texture described as “exsolved” might have been caused by crystallographically controlled replacement, but the zoning sequence described below is not consistent with such an origin. The possibility that most of the complex exsolution-induced textures might have been caused by deformation was rejected, as these placer-derived par-

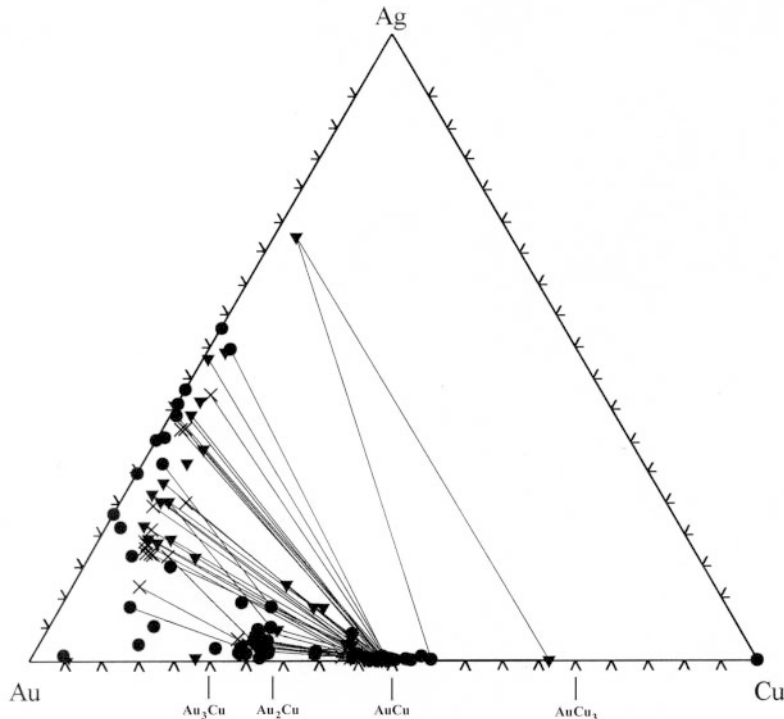


FIG. 5. Data (in at.%) for the compositions of the principal phases within gold particles from Wheaton Creek and the 15 Mile showing. X: exsolved phase, inverted triangle: blebby phase, •: massive phase. The tie-lines join phases considered to be in equilibrium.

ticles showed close to the lowest degree of deformation possible, and the formation or preservation of zoning is inconsistent with general deformation. The possibility of localized deformation cannot be rejected, but the similarity of intergrowth textures near the center to those at the edge of particles at all scales suggests that deformation is rare in these samples. For placer particles with this low level of general deformation, the localized deformation is generally concentrated near the edge of the particle (Knight *et al.* 1999).

Most of the particles have some areas (in a few cases even the whole particle) where no textural features can be recognized. These homogeneous areas are described as massive (*e.g.*, Fig. 3c, grey area at top right of particle). In composite particles, the massive areas usually occur toward the edge of the particle (*e.g.*, Fig. 3d, grey area at the lower left of the particle).

Most particles contain areas of one or both of two types of inhomogeneities, blebby and exsolved. Areas

described as blebby are similar to massive areas in that they are internally homogeneous. They differ from massive areas in that they are much smaller. They may be surrounded by massive areas, where they are recognized by their different composition, or may either lie on the boundaries or be surrounded by exsolved areas, where they are recognized by their homogeneity. In the latter case, two blebs of different compositions can occur in the same particle (Fig. 3e, grey and white areas dominating the neck in the particle). In particles dominated by exsolved areas, the blebs usually occur toward the particle edge, whereas in particles with massive and exsolved areas, the blebs are preferentially concentrated toward the boundary between the two areas. In some cases, the blebby areas merge with the massive areas (Fig. 3d, black and grey areas on the left edge of the particle).

Exsolution textures are common. In particles that display exsolved areas, both the contrasting compositions and variable orientations of the exsolution-induced intergrowths outline grain boundaries (Fig. 3b, in particular at the bottom right of the particle; Fig. 4d). Exsolution intergrowths can occupy the whole particle, but in composite particles, they usually occupy only the central portion. Grains showing exsolution-induced intergrowths also serve to outline massive grains and blebs (Fig. 3c, grey area to the left of the particle). Exsolution intergrowths are diverse in their expression (Figs. 3, 4). Thin (occasionally thick) straight, nearly parallel-sided (but ultimately tapered) exsolution lamellae are common, but thicker lens-like and more irregular forms also are found. The latter resemble blebs in some cases. Many exsolution lamellae are composites of multiple events of exsolution. This is most clearly seen in BSE images (Fig. 4a). Different orientations of the lamellae, both in different grains and within exsolution lamellae, create the impression of a network (Figs. 3b, 4c; *cf.* Murzin & Sustavov 1989). Examples of the composition of these textural types are reported in Table 1. In Figures 5 and 6, the data are shown along with tie-lines joining phases considered to be in equilibrium.

BSE imaging of the particles confirms the observations in reflected light. However, it also shows that the degree of exsolution is far greater than revealed by light microscopy (*cf.* Figs. 3a, 4a). Exsolution can occur to the submicrometer scale (Fig. 4). The BSE imaging allows features at the submicrometer scale to be considered during the selection of sites for analysis. Many but not all such sites were checked by BSE imaging, so it is certain that some of the compositions reported represent bulk compositions.

Zoning is crudely developed in composite particles. The exsolved areas lie toward the center, with massive areas on their outer edge. The blebby areas lie near the edge of the exsolved area, either along exsolved grain boundaries or between exsolved and massive areas (Figs. 3d, 4c). In particles that are dominantly massive,

TABLE 1. REPRESENTATIVE COMPOSITIONS OF GOLD COPPER ALLOY, WHEATON CREEK, BRITISH COLUMBIA

in Fig.	444-02-18 X 3a	444-02-18MX 3a	444-02-18T 2a lath, 3a	444-02-20Q? 3b	444-02-20 B 3b	444-02-20MX 3b
tone	center *	grey	white	black with grey	grey	white
texture	exsolved	exsolved	bulk	exsolved	exsolved	exsolved
mineral	Au,Cu ?	AuAg near Z		Au,Cu ?	AuCu	AuAg near Z
Au wt%	85.61	85.86	80.06	85.39	76.82	86.43
Ag	1.77	10.71	0.43	1.46	0.13	10.74
Hg	0.00	0.00	0.00	0.03	0.02	0.04
Cu	12.32	4.17	19.57	12.78	23.25	3.10
total	99.70	100.74	100.06	99.66	100.20	100.31
Au at. %	67.39	72.55	56.58	66.86	51.53	74.72
Ag	2.55	16.53	0.56	2.09	0.15	16.95
Hg	0.00	0.00	0.00	0.02	0.01	0.04
Cu	30.07	10.93	42.86	31.02	48.31	8.30
in Fig.	506-01-07M 3c	506-01-07T 3c	506-01-07N 3c	506-01-07B 3c	444-01-12 X 2c *	444-01-12MX 2c *
tone	center *	right center *	lower left	upper left	grey	white
texture	exsolved	finely exsolved	bulk	white	black	exsolved
mineral	Au,Cu ?		AuAg	AuCu	AuCu	AuAg
Au wt%	85.36	82.29	85.13	77.61	76.25	74.16
Ag	1.38	0.79	12.04	0.17	0.11	24.91
Hg	0.00	0.00	0.15	0.00	0.00	0.08
Cu	13.23	16.93	3.12	22.32	23.08	1.24
total	99.97	100.01	100.44	100.10	99.44	100.39
Au at. %	66.23	60.41	72.80	52.75	51.53	60.02
Ag	1.96	1.06	18.79	0.22	0.13	36.80
Hg	0.00	0.00	0.13	0.00	0.00	0.06
Cu	31.81	38.53	8.29	47.03	48.34	3.12

* Analysis point lies within the field of view covered by the figure cited. The other compositions are representative of the phases in the figure, but the analyses were made outside the field of view. Results of electron-microprobe analyses.

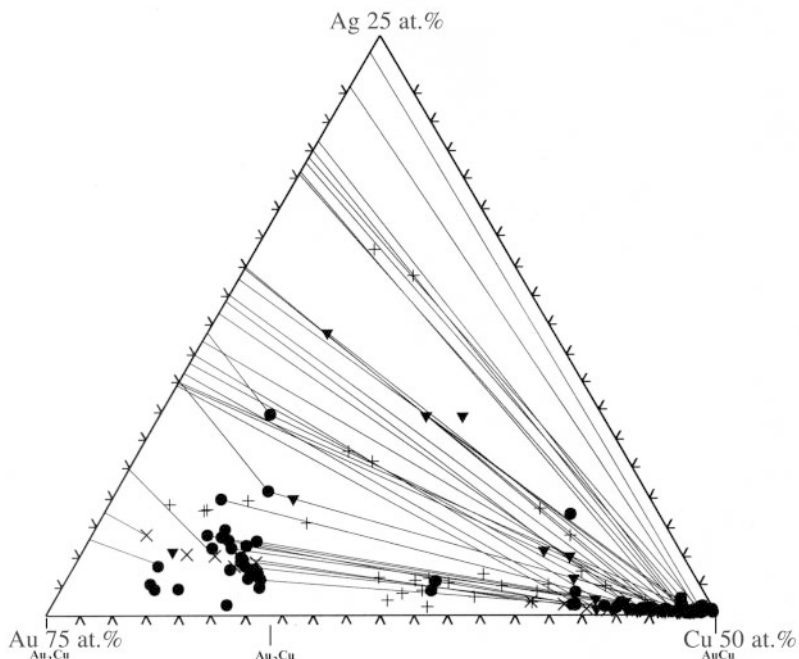


FIG. 6. Details of Figure 5 intended to illustrate the clustering around AuCu and the composition Au_2Cu , the relationship of AuCu to Au_2Cu , and the trends used to generate the formulas for AuCu and Au_2Cu (see text). For compositions near AuCu, there is overlap of points representing blebby, massive and exsolved material. Symbols as for Figure 5 with the addition of +, representing bulk compositions (in at. %) of mixed phases.

blebby areas can occur along the edges of the particles. For Au–Cu compositions between 50 and 60 at. % Au, massive phases are generally closest to 50 at. % Au (mean: $Au_{1.0}Cu_{0.97}Ag_{0.003}$), followed by blebby and exsolved phases with increasing Au content. Along the outer margin of some particles, one of two types of zones is found. One is a thin but incomplete zone consisting of a massive phase. Usually, this massive phase can be identified as part of the sequential zoning discussed above and is thus called the edge phase (Fig. 7). A few particles from Wheaton Creek display the second type of zone, which consists of either a thin porous zone or a thin discontinuous gold-rich phase. The characteristics of the porous second type of zone are consistent with the features formed by the leaching of Ag, Cu and Hg from particles of gold alloy in the surficial environment and referred to as rims (Knight *et al.* 1999). The composition of the massive phases at the edge and the residual gold rims are reported in Figure 7.

Numerous mineral inclusions in gold and attachments to the gold were seen. A detailed study of the inclusions was not undertaken. The following identifications are based on results of qualitative EDS analyses. From the 15 Mile sample, diopside, Fe-poor, Ca-rich garnet (grossular?), a Ca–Al silicate (epidote?

vesuvianite?), Ni–Sb alloy, chalcocite, bornite and a Pt, Pd, Cd, S mineral or minerals. The following were identified from the Wheaton Creek area: magnetite, high-Mg–Fe silicate (pyroxene? olivine?), Mg silicate (serpentine?), calcite, chalcocite, CoNiAs mineral, CuFeS (bornite?). Large nuggets of copper also are found in the Wheaton placer.

In order to further limit the conditions of formation of the 15 Mile sample, fluid-inclusion studies were undertaken on three samples of rodingite and one of serpentinite from the dump and ore bin. No gold was seen in these samples but, as discussed above, we are certain that the gold is hosted in part by the rodingites. The fluid inclusions measured in this study occur in grossular (three samples; total of 19 inclusions) and diopside (one sample, total of nine inclusions). The fluid inclusions have a restricted single grouping of homogenization temperatures (T_h) between 230 and 280°C (28 determinations). Ice-melting temperatures (T_m) form a single grouping between -0.2 and -1.4°C (21 determinations), indicating low salinities in the range 1–2 wt% eq. NaCl. Eutectic (T_e : first melting) temperatures, mainly in the -30 to -43°C range, rarely to -54°C , indicate that Mg or possibly Mg and Ca may be present. The fluid is relatively CO_2 -poor, as indicated by the

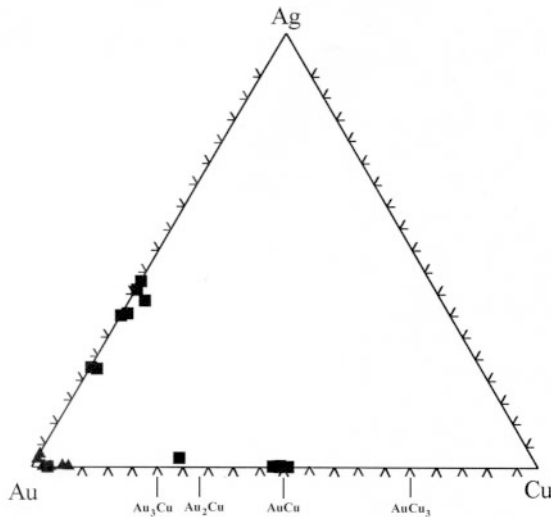


Fig. 7. Composition of the phases (in at.%) comprising a rim (triangle), apparently generated in the surficial environment, or the edge (square) of the hydrothermal gold particles whose principal phases are plotted in Figure 5. The composition of the edge phase falls in locations expected as a result of low-temperature precipitation. The composition of the rim material is near the range expected by leaching of Cu, Ag, and Hg in the surficial environment.

absence of clathrate formation or clathrate-melting events.

INTERPRETATION

Figures 5 and 6 illustrate the analytical results represented in Table 1, grouped by texture type (blebby, massive, or exsolved phase), with tie lines linking the phases considered to be in equilibrium. The exsolution texture in some particles is simple, and consists of two phases (Fig. 3c), whereas in others, the texture is more complex (Fig. 4a). Upon analysis, these complex textures can be broken down into a series of binary pairs of apparently three end-member compositions. These end-members, together with the massive and blebby phases, form the clusters and trends seen in Figures 5 and 6 (*e.g.*, around compositions AuCu and Au₂Cu). Bulk compositions of fine intergrowths not amenable to single-phase analysis (Table 1, Fig. 4d) usually fall on the tie-line zones, shown for example in Figures 6. This coincidence suggests that the fine intergrowth results from a late-stage or weakly developed exsolution of known phases rather than of some unknown phase.

These results were combined with the results of Pokrovskii *et al.* (1979) to generate a low-temperature phase diagram for the system Au–Ag–Cu (Fig. 8, near 25°C and 1 atm, after sufficient time for equilibration).

This diagram is considered to represent the composition of the phases present with consideration given to the spatial limit of X-ray micro-analysis and to evidence of submicrometer-scale exsolution (where data are available). The most important features of Figure 8 are the recognition of a possible three-phase field involving AuCu, Au₂Cu and Au₃Ag_{0.71}Cu_{0.23} (referred to as Z for convenience), the observation that the analyzable gold-rich Au–Cu alloy in this study has a composition close to that represented by Au₂Cu rather than the expected stoichiometric composition Au₃Cu representative of the mineral auricupride, and the presence of a two-phase region on the Au side of the Au₂Cu – Z join. The low-Au part of the system (Fig. 8) is in general agreement with the theoretical phase-relationships of Kikuchi *et al.* (1980), shown in Figure 1. For the medium- and high-Au part of the system, the agreement is very poor, but what is shown likely applies to very different temperatures (240° and 25°C). The two tie-lines reported by Bird *et al.* (1991) are in agreement with Figure 8. For the three-phase region, the bounding compositions on the Au–Cu join were determined from the data illustrated in Figure 6. The mean composition for massive phases around Au_{1.0}Cu_{0.97}Ag_{0.003} is considered to represent the maximum deviation from stoichiometry on the Au side of AuCu. This deviation from stoichiometry toward Au is much less extensive than that reported by Okamoto *et al.* (1987) for experimental systems, and closer to that reported by Murzin & Sustavov (1989) for natural AuCu. However, for bulk compositions of finely exsolved phases (+ in Fig. 6) near the join AuCu–Au₂Cu (and trending toward AuCu), the maximum Au content corresponds to the maximum deviation for Au-enriched AuCu (II) given by Okamoto *et al.* (1987). This deviation and the trend toward AuCu from finely exsolved to blebby to massive phases are considered to represent the effect of a change in temperature with time.

The composition at the triple point, Z (Fig. 8), was chosen to correspond to the point on the edge of the exsolved area which 1) is joined to AuCu, 2) is limited by one tie-line to Au₂Cu, the trend in compositions leading away from Au₂Cu, and 3) lies on the curve corresponding to the maximum Cu in Au–Ag alloy compositions, as defined by the boundary between the massive and blebby phases (Fig. 5). Because the exsolution lamellae analyzed are considerably larger than the minimum size of exsolution present (which are nearest equilibrium?), the composition at Z (Au₃Ag_{0.71}Cu_{0.23}) is almost certainly too high in Cu (Fig. 5). This choice is based on a limited search for exsolution textures. Murzin & Malyugin (1983) used etching and electron microscopy on natural samples of gold alloy to develop a curve for the boundary between phases showing exsolved and homogeneous phases for the Au end of the Au–Ag–Cu phase diagram (Fig. 8). Their curve is in agreement with the curve based on our interpretation in that both suggest that Cu is more

soluble in Au–Ag alloy than is Ag in Au–Cu alloy. The curve of Murzin & Malyugin (1983) lies nearer to the graph axes and is probably a truer representation of the equilibrium compositions at low temperature (Fig. 8). Their curve suggests that the saturation value of Cu for Z lies between 1.75 and 2.25 at.% Cu.

The composition near Au_2Cu is constrained by the trend in the compositions from AuCu toward Au_2Cu and the trend in the compositions of Au_2Cu toward Z (Fig. 6). The trend toward Z is reinforced by the linear distribution of bulk compositions between Au_2Cu and Z. The following observations are considered to support the conclusion that Au_2Cu really corresponds to the composition of a phase rather than an analytical error. Natural compositions near Au_2Cu are reported as stoichiometric Au_3Cu , but are commonly better represented as having a composition near Au_2Cu . For example, Murzin & Sustavov (1989) reported naturally occurring stoichiometric AuCu and AuCu_3 after a careful selec-

tion of samples, but described Au_3Cu as deviating from stoichiometry. Using their numbers, 12.25 wt% Cu (between their reported 12.0 and 12.5 wt% Cu), Ag at 1.5 wt% (<2 wt% reported), with the balance as gold, the formula for the alloy is $\text{Au}_2\text{Cu}_{0.881}\text{Ag}_{0.064}$ (total atoms 2.945), which is equivalent to $\text{Au}_3\text{Cu}_{1.322}\text{Ag}_{0.095}$ (total atoms 4.417). The total number of atoms shows that this composition is closer to Au_2Cu than Au_3Cu in stoichiometry. This composition falls close to the trend line between Z and Au_2Cu , near the composition Au_2Cu (Fig. 6). A further example comes from Knipe & Fleet (1997). Their reported range in composition for Au_3Cu (their Fig. 1) covers Au_2Cu at the high-copper end. Finally, the presence of exsolved areas, blebby areas and tie-lines on the high-Au side of the join Au_2Cu –Z join (Figs. 5, 6) further supports the conclusion that Au_2Cu is the composition of a phase. It is possible that this composition is caused by the presence of unrecognized or unexposed exsolution-related intergrowths. Such

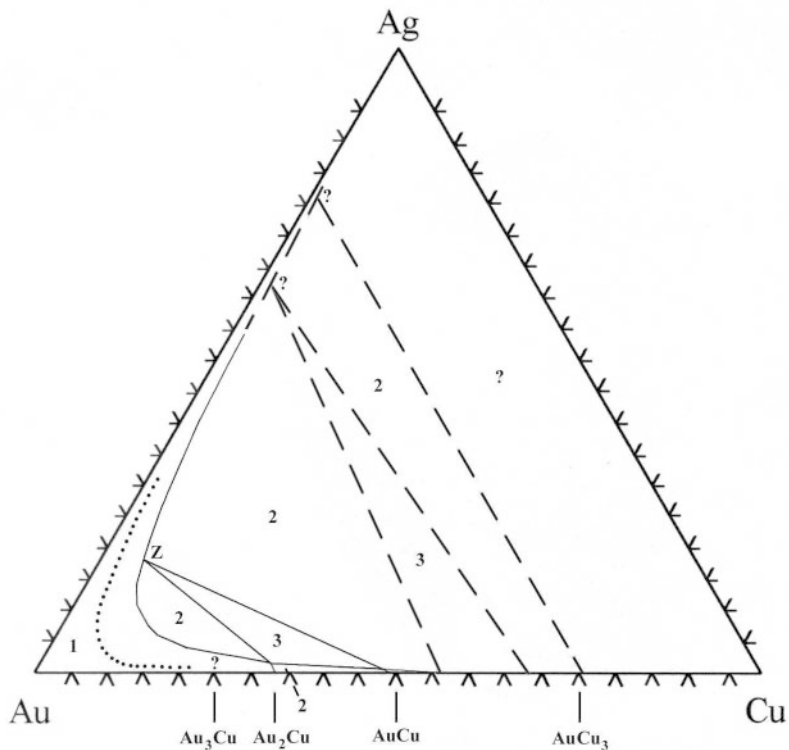


FIG. 8. The proposed phase-diagram for the system Au–Cu–Ag at less than 100°C based on data from this study (solid lines) and Pokrovskii *et al.* (1979) (dashed lines) from the Zolotaya Gora deposit in the Urals. Data from Murzin & Malyugin (1983) (dotted line) from the Urals region illustrate the lowest Cu content of gold still showing exsolution reported to date. Areas marked 3 are three-phase, and those marked 1 are one-phase regions, whereas ? indicates points of uncertainty in detail. The composition at Z is $\text{Au}_3\text{Ag}_{0.71}\text{Cu}_{0.23}$. The composition limit established in this study for one side around Au_2Cu is $\text{Au}_2\text{Cu}_{0.962}\text{Ag}_{0.045}$, and at AuCu, it is $\text{Au}_{1.0}\text{Cu}_{0.971}\text{Ag}_{0.003}$.

unrecognized or unexposed intergrowths are considered, in part, to account for the trend from AuCu toward Au₂Cu and between Au₂Cu and Z. No such trend in the data is seen between Au₂Cu and Au₃Cu (Figs. 5, 8). Au₂Cu seems to represent the stoichiometry of a valid phase. It thus seems, for the data presented in this study, that the pertinent debate is whether the Au₂Cu composition reported here is part of the extended but unsampled compositional range of auricupride (Au₃Cu) (which may become restricted to stoichiometric Au₃Cu with a decrease in temperature), or whether Au₃Cu decomposes into a two-phase region between Au and Au₂Cu. If stoichiometric Au₃Cu is indeed the low-temperature phase, then it would be expected that for the appropriate bulk-composition, a trend and clustering of compositions similar to that around Au₂Cu would be apparent on the excess-Au side of Au₃Cu.

Synthetic alloys do not provide an answer because the range in composition of each phase is very large for the temperatures studied (*e.g.*, 38.5 to 63 at.% Cu for AuCu, 10 to 38.5 at.% Cu for Au₃Cu; Okamoto *et al.* 1987). The details of the phase diagram around Au₃Cu are imperfectly known (Okamoto *et al.* 1987), and in-

clude the possibility of a two-phase region around Au₃Cu. Considering that the properties of Au₃Cu were determined from data at the limit of the experimental method, it would be expected that Au₃Cu would have the largest range in composition. Perhaps a range in bulk composition closer to Au than that studied here would define the phases around Au₃Cu. A review of published data for natural compositions of Au–Cu alloy in this region shows that they do fall between Au₂Cu and Au₃Cu, but they are too few in number, and it was not possible to evaluate whether the compositions represent single or multiple phases (Fig. 2). Our findings and those of Murzin & Sustavov (1989) both show at least a two-phase region on the Au–Ag side of Au₂Cu–Au₃Cu, but from the very limited data in their study, the Au–Ag phase may be joined to Au₂Cu, not Au₃Cu.

In an attempt to clarify this problem, 258 analyses of Au–Ag alloy particles from placers in southern British Columbia in which high (>0.6 at.%) Cu values were reported were plotted (Fig. 9). These particles were checked by optical microscopy and occasionally checked by BSE imaging for exsolution textures before analysis. Although none were recognized, the work of

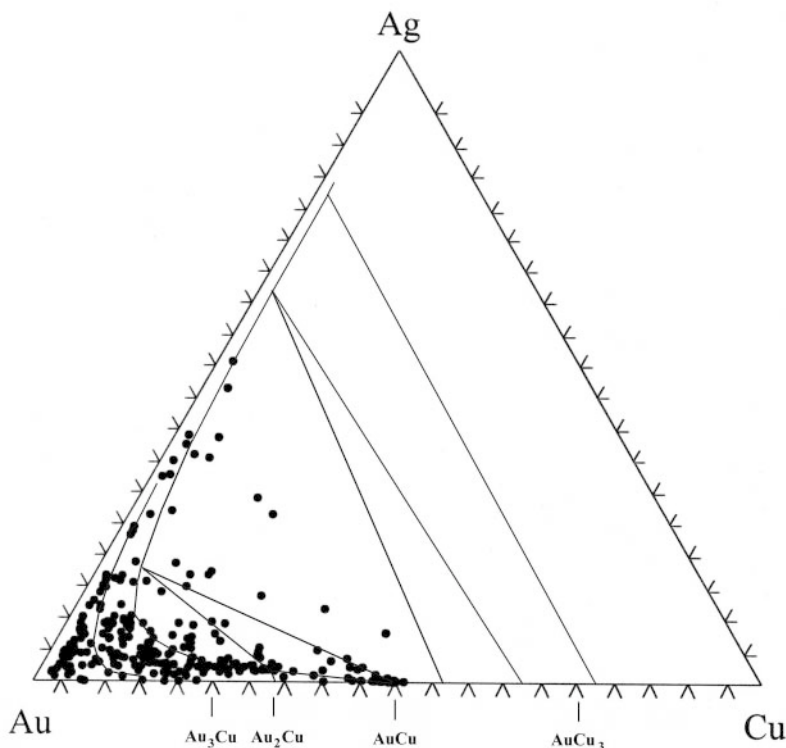


FIG. 9. The analysis of 258 Cu-rich phases from placer gold particles. Most particles are from southern British Columbia in the Coquihalla District. Exsolution was checked using reflected light but, as the scatter in the center of the diagram shows, was not always recognized. For convenience, the phase boundaries from Figure 8 also are displayed.

Murzin & Malyugin (1983) and our findings suggest that more care is required to identify exsolution textures in compositions plotting toward the Au apex. There is no suggestion of a clustering around Au_3Cu in Figure 9, nor of a gap in the data between Au and Au_2Cu . If anything, the data suggest a continuum between Au and Au_2Cu . The step in the data away from the Au–Cu axis around 80 at.% Au is noted, but its significance is unclear.

The work of Knipe & Fleet (1997, Fig. 2) provides further data. The Au–Cu alloy compositions they studied are considered to have formed at 130°C, where the departure from stoichiometry with respect to Au_3Cu should be less than the variation observed in this study, in which the gold is considered to have initially formed between 230° and 280°C. They reported a gap between Au and Au_3Cu . They also reported a compositional asymmetry with respect to Au_3Cu , with the Au-rich side corresponding to stoichiometric Au_3Cu and the Cu-rich side falling near Au_2Cu . The quality of the polish and size of phases shown in their Figure 2 suggest that some of these contradictions may be the result of analytical problems.

The small massive grains at the extreme edge of some of the particles are attributed to the composition of the last phases to form at the lowest temperature (Fig. 7, edge). The edge compositions around AuCu are very close to being stoichiometric, as would be expected. The edge compositions on the Au–Ag join have lower Cu values than those expected from Figure 8, and fall within the line taken from Murzin & Malyugin (1983). The remaining compositions are suggestive, but too few in number to be definitive. The only edge composition near Au_3Cu falls between Au_3Cu and Au_2Cu , and is suggestive of a change from Au_2Cu . A few edge compositions fall near the Au apex on the Au–Cu join. Some of the compositions marked as rim phases fall near these points. The higher-than-expected Cu values (around 5 at.% Cu) for a rim phase suggest that these phases may be misidentified and are possibly edge phases (the possibility of contamination excepted). Along the Au–Cu axis, the curve of Murzin & Malyugin (1983) lies very close to the Au–Cu axis and covers the area around the Au apex. Unfortunately, there are only two points on their curve beyond 12 at.% Cu. Both of these compositions lie away from the Au–Cu axis and refer to two-phase mixtures. Their composition around 12 at.% Cu also represents the highest Cu content for a single-phase particle. What evidence exists is thus suggestive of a two-phase field on the Au side of Au_3Cu , but the evidence is far from conclusive.

In this study, mercury reaches 1.2 at.%, with most values falling below 0.4% Hg. This is not sufficient to change the geometry of the Au–Ag–Cu phase diagram. Mercury is close to or below detection limits for alloy compositions with >15 at.% Cu (Ag less than about 5 at.%). The Hg values are highest in low-Cu Au–Ag alloy, which is in agreement with the findings of

Pokrovskii *et al.* (1977), who reported Hg values up to 10 wt%. There is a weak correlation between increases in Ag and in Hg. A similar but strong correlation was reported by Pokrovskii *et al.* (1977).

DISCUSSION

Knipe & Fleet (1997) have suggested that the presence of various Au–Cu alloy compositions represents a change in the bulk composition of the system with time, but this is not considered to be necessarily the case. For this study, at least the textures and zoning shown by both reflected-light images (Fig. 3) and the BSE images (Fig. 4) can be understood with reference to the proposed phase-diagram (Fig. 8). These features are attributed to a combination of exsolution and precipitation as the composition of the phases changed with time within the one-, two- and three-phase fields. Because the solvi move rapidly with temperature in the Au–Cu–Ag phase diagram (Kikuchi *et al.* 1980), we expect that a change in temperature rather than in composition is responsible for variations with time. On the basis of Figure 3e as an example and under the assumption that the bulk composition of the fluid remained constant, the first gold to precipitate plots in a one-phase field. As the temperature dropped, the gold passed into a two-phase field, at which time the blebby areas were precipitated, and the single phase started to exsolve. With a further drop in temperature, the compositions diverged further, one to be precipitated as the thin massive outer phase on the particle, and the other at a different site. At the same time, exsolution within the blebby area at the micrometer to submicrometer level may have started, and the composition of exsolution lamellae making up the original single phase will have diverged. A more complex example of the exsolution sequence can be seen in Figures 3a and 4a, where three distinct phases are exsolved. In zoned particles, the appearance of the blebby phases may represent the temperature at the beginning of precipitation in a two-phase field. With this model, the data of Knipe & Fleet (1997) can be interpreted to represent precipitation from (or reaction with) a low-temperature fluid that varied in composition with location, but was essentially constant with time. For example, their phase 2 could have formed with their phase 3 in a two-phase field. This is not to say that changes in fluid composition did not take place, only that the changes were smaller than those seen by the phase separation. This model also suggests that the Wheaton sample comes from a lode formed at a higher temperature than at the 15 Mile showing.

The curve of Murzin & Malyugin (1983) is taken to represent the maximum Cu soluble in Au–Ag alloy before exsolution takes place (Figs. 6, 10). The amount of Cu in Au–Ag alloy from areas where a Cu–Au alloy is not present is given by the other curves in Figure 10. The figures and data from which these curves were taken show two types of “maxima”: a maximum line below

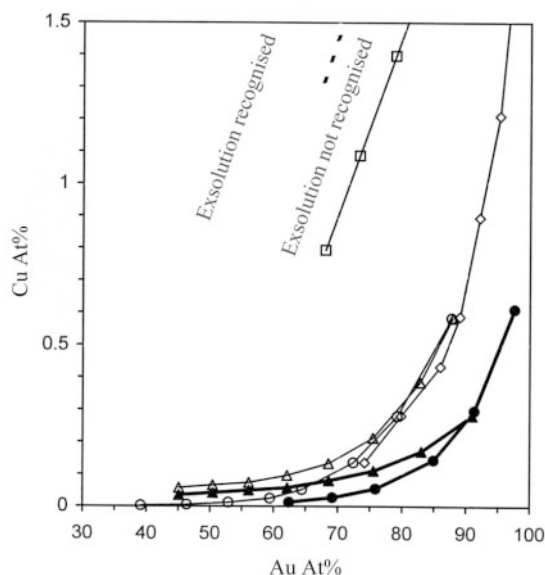


FIG. 10. Limits to the Cu content in the most common Au–Ag alloy compositions. The dashed line is from Murzin & Malyugin (1983), established for material from the Urals region. It separates compositions for which exsolution has been observed (below dashed line) from those where it has not. There are few data-points between the dashed “exsolution” line and the “upper limit” line (open squares) for the Urals region (226 analytical data from Murzin & Malyugin 1983). The upper limit curve for the Yano–Kolyma region is shown by open diamond symbols (from Murzin & Malyugin 1983) and open circles (approximately 220 analytical data from Samusikov & Petrova 1983). The upper limit curve for the Yukon and British Columbia is shown by the black triangles (>3500 analytical data from Knight & McTaggart 1990, McTaggart & Knight 1993, Knight *et al.* 1999). Open symbols and thin lines are upper limits, solid symbols and thick lines are maximum values; see text.

which most but not all points fall, and the upper limit, a line above which no points fall. The upper-limit line is taken to represent the absolute maximum amount of Cu found in grains of Au–Ag alloy for that region. The upper-limit line for the Urals shows that grains of Au–Ag alloy from this region do indeed have higher-than-normal Cu. The upper-limit lines for the Yano–Kolyma region of Russia and for British Columbia – Yukon are essentially the same. At first glance, these curves suggest that these lines, rather than the curve of Murzin & Malyugin (1983), represent the maximum Cu content possible in an Au–Ag alloy. However, deposits that host Au–Ag alloy but no Au–Cu alloy are formed over the same range in temperature as the deposits hosting a Au–

Cu alloy. The difference between the two assemblages appears to have more to do with the fluid precipitating the metals than with an error in the phase diagram. Invariably, grains of Au–Cu alloy are associated with native metals, sulfides are not common, and a substantial proportion of them are low-sulfur varieties such as bornite and chalcocite (*e.g.*, Pokrovskii *et al.* 1979, this study). In gold deposits without grains of Au–Cu alloy, the Au–Ag alloy is invariably associated with significant amounts of the common sulfides such as pyrite and arsenopyrite (Boyle 1979). We suggest that the amount of Cu in Au–Ag alloy from deposits with no Au–Cu alloy is controlled by the presence of additional elements, in particular sulfur, in the system. The Yano – Kolyma and British Columbia – Yukon curves may represent the undersaturation of Cu in Au–Ag alloy caused by this difference, and thus contain information about the process of formation of a deposit, not the Cu limit in Au–Ag alloy compositions.

CONCLUSIONS

The composition and textures of natural alloy that result from long periods of equilibration at low temperatures (near 25°C?) can be used to construct a phase diagram for the system Au–Cu–Ag. The most important features of the diagram proposed from the results of this study are the recognition of a three-phase field between AuCu ($\text{Au}_{1.0}\text{Cu}_{0.971}\text{Ag}_{0.003}$), Au_2Cu ($\text{Au}_2\text{Cu}_{0.962}\text{Ag}_{0.045}$), and $\text{Au}_3\text{Ag}_{0.71}\text{Cu}_{0.23}$, the presence of a two-phase region for alloy compositions on the Au side of this three-phase field, and the observation that the compositional range around Au_2Cu is restricted. AuCu is nearly stoichiometric. Even after taking into account the problem of micrometer-scale exsolution, the evidence suggests that the compositions around Au_2Cu are representative, within the limits of this study. The details of the phase diagram between compositions Au, Au_3Cu and Au_2Cu are unclear. Whether there is solid solution over the range Au, Au_3Cu and Au_2Cu , or whether there are miscibility gaps, remains unresolved. The study of exsolution intergrowths by Murzin & Malyugin (1983) sets a limit for the amount of Ag in Au–Cu alloy and the amount of Cu in Au–Ag alloy beyond which exsolution occurs. The values for Cu in Au–Ag alloy are low, but not as low as those reported for Au–Ag alloy from deposits where Au–Cu alloy is absent. These very low values are considered to reflect the chemical composition of the fluid associated with deposition, and do not reflect the phase diagram. The extensive exsolution-induced textures and their relation to the blebby and massive textures are explained by combining the phase diagram with the significant shift in the solvi position with temperature in this system. For example, blebby textures are considered to occur as precipitation changes from a one- to a two-phase field. Mercury is preferentially partitioned into low-Cu, high-Ag gold alloy.

ACKNOWLEDGEMENTS

Dr. K.C. McTaggart is acknowledged for recognizing the significance of Cu-rich gold and for encouraging this study. We thank J. Schussler for the Wheaton sample, and Sun Min and K. Wilkie for help in collecting the 15 Mile sample. The reflected-light photographs were taken by E. Montgomery. Y. Douma and B. Cranston provided high-quality technical assistance. J. McIntosh graciously helped with finding and translating some of the Russian literature. I. Zergsky translated the remainder of the Russian literature. Funding for the analyses was provided by the British Columbia Ministry of Energy, Miners and Petroleum Resources and Westmin Resources Limited. Thanks to S. Knipe and E. Essene, whose reviews greatly improved this manuscript.

REFERENCES

- BARRETT, C.S. & MASSALSKI, T.B. (1980): *Structure of Metals* (3rd ed.). Pergamon Press, New York, N.Y.
- BIRD, D.K., BROOKS, C.K., GANNICOTT, R.A. & TURNER, P.A. (1991): A gold-bearing horizon in the Skaergaard intrusion, east Greenland. *Econ. Geol.* **86**, 1083-1092.
- BOWLES, J.F.W. (1984): The distinctive low-silver gold of Indonesia and East Malaysia. In *Gold 82: The Geology, Geochemistry and Genesis of Gold Deposits* (R.P. Foster, ed.). *Geol. Soc. Zimbabwe, Spec. Publ.* **1**, 249-260.
- BOYLE, R.W. (1979): The geochemistry of gold and its deposits. *Geol. Surv. Can., Bull.* **280**.
- CAIRNES, C.E. (1930): The Serpentine Belt of Coquihalla Region, Yale District, British Columbia. *Geol. Surv. Can., Sum. Rep.*, 1929, 144A-195A.
- DOUMA, Y.L. & KNIGHT, J.B. (1994): Mounting samples in methyl methacrylate for SEM and EMP studies. *J. Sed. Res.* **A64**, 675-677.
- DOWDELL, R.L., JERABEK, H.S., FORSYTH, A.C. & GREEN, C.H. (1943): *General Metallography*. John Wiley & Sons, New York, N.Y.
- HOLLAND, S. (1940): Placer gold deposits: Wheaton (Boulder) Creek, Cassiar district, northern British Columbia. *B.C. Dep. Mines, Bull.* **2**, 1-44.
- KIKUCHI, R., SANCHEZ, J.M., DE FONTAINE, D. & YAMAUCHI, H. (1980): Theoretical calculation of the Cu-Ag-Au coherent phase diagram. *Acta Metall.* **28**, 651-662.
- KNIGHT, J. & MCTAGGART, K.C. (1989): Composition of gold from southwestern British Columbia, a progress report. *B.C. Dep. Energy, Mines, Petroleum Resources, Geol. Fieldwork 1988, Pap.* **1989-1**, 387-394.
- _____ & _____ (1990): Lode and placer gold of the Coquihalla and Wells areas, British Columbia (92H, 93H). *B.C. Energy, Mines, Petroleum Resources, Exploration in British Columbia 1989*, 105-118.
- _____, MORISON, S.R. & MORTENSEN, J.K. (1999): The relationship between placer gold particle shape, rimming, and distance of transport as exemplified by gold from the Klondike district, Yukon Territory, Canada. *Econ. Geol.* **94**, 635-648.
- KNIFE, S.W. & FLEET, M.E. (1997): Gold-copper alloy minerals from the Kerr mine, Ontario. *Can. Mineral.* **35**, 573-586.
- KOGACHI, M & NAKAHIGASHI, K. (1980): Phase relations in the $\text{Cu}_3\text{Ag}_{1-x}\text{Au}_x$, $\text{Ag}_3\text{Au}_{1-x}\text{Cu}_x$, $\text{Au}_3\text{Cu}_{1-x}\text{Ag}_x$ ternary system. *Japan. J. Appl. Phys.* **19**, 1443-1449.
- KUZNETSOV, YU.A., PANOV, B.S., SAMOILOVICH, L.G. SHARKIN, O.P. & LAZARENKO, E.K. (1977): Cuprous gold in the Donetsk Basin. *Vopr. Reg. Genet. Mineral., S'ezde Ukr. Mineral. Obshchest.* (E.K. Lazerenko, ed.). Naukova Dumka, Kiev, USSR (59-63; in Russ.). (*Chem. Abstr.* **88**:173534x).
- MAO, S.H. & LIU, T.X. (1984): A study of gold-copper minerals using the electron probe. *J. Phys., Colloq.* **C2**, suppl. **45**, 631-634.
- MCTAGGART, K.C. & KNIGHT, J.B. (1993): Geochemistry of lode and placer gold of the Cariboo district, B.C. *B.C. Dep. Energy, Mines, Petroleum Resources, Open File 1993-30*, 1-26.
- MONGER, J.W.H., PRICE, R.A. & TEMPLEMAN-KLUIT, D.J. (1982): Tectonic accretion and the origin of the two major metamorphic and plutonic belts in the Canadian Cordillera. *Geology* **10**, 70-75.
- MURZIN, V.V., KUDRYAVTSEV, V.I., BERZON, R.O. & SUSTAVOV, S.G. (1987): Cupriferous gold in rodingitized zones. *Geol. Rudn. Mestorozhd.* **29**(5), 96-99 (in Russ.).
- _____ & MALYUGIN, A.A. (1983): New data on the instability of natural solid solutions of the gold-silver-copper system at temperatures below 350°C. *Dokl. Acad. Sci. USSR, Earth Sci. Sect.* **269**, 723-724.
- _____ & MOLOSHAG, V.P. (1986): Typomorphism of gold of pyrite deposits of the Urals. In *Geochemistry and Mineralogy of Primary and Secondary Haloes* (N.A. Grigor'yev, V.V. Murzin & V.N. Savonov, eds.). *Akad. Nauk SSSR - Uralskii Nauchmit Tsentr. Sverdlovsk*, 100-107 (in Russ.). (*Chem. Abstr.* 107:26229j).
- _____ & SUSTAVOV, S.G. (1989): Solid-phase transformation in native cupriferous gold. *Izv. Akad. Nauk SSSR, Ser. Geol.* **11**, 94-104 (in Russ.). (*Chem. Abstr.* **114**(2):9751a).
- NOVGORODOVA, M.I. & TSEPIN, A.I. (1976): Phase compositions of cupriferous gold. *Dokl. Acad. Sci. USSR, Earth Sci. Sect.* **227**, 121-123.

- OKAMOTO, H., CHAKRABARTI, D.J., LAUGHLIN, D.E. & MASSALSKI, T.B. (1987): The Au–Cu (gold – copper) system. *Bull. Alloy Phase Diagram* **85**, 454-474.
- PETROVSKAYA, N.V. & NOVGORODOVA, M.I. (1980): Heterogeneity of native gold and some problems relating to stability of natural solid solutions of metals. *In Inhomogeneity of Minerals and Crystal Growth. Proc. XI Gen. Meeting (Moscow, 1978), Int. Mineral. Assoc.*, 76-86, 296-297, 330 (in Russ.).
- _____, _____, FROLOVA, K.E. & TSEPIN, A.I. (1977): Nature of the nonuniformity and phase composition of endogenic segregations of native gold. *Neodordnost Miner. Tonkie Miner. Smesi*, (F.V. Chukhrova & N.V. Petrovskaya, eds.). Nauka, Moscow, Russia (16-27; in Russ.). (*Chem. Abstr.* **89**:046532r).
- POKROVSKII, P.V. & BERZON, R.O. (1975): Composition of copper and silver gold from the deposit Zolotaya Gora. *Ezheg., Inst. Geol. Geokhim., Akad. Nauk SSSR, Ural. Nauchn. Tsentr.* **1974**, 94-97 (in Russ.). (*Chem. Abstr.* **86**:7236r).
- _____, MURZIN, V.V., BERZON, R.O. & YUNIKOVA, B.A. (1979): Mineralogy of native gold from the Zolotaya Gora deposit. *Zap. Vses. Mineral. Obshchest.* **108**, 317-326 (in Russ.). (*Chem. Abstr.* **91**:143452p).
- _____, SANDLER, G.A., CHESNOKOV, B.V., BERZON, R.O., ALEKSANDROV, A.I., BARANNIKOV, A.G. & KHRYPOVA, R.G. (1977): Characteristics of distribution of silver, iron, copper and bismuth in native gold of some Ural deposits. *Tr. In-ta Geol. Geokhimii Ural'sk, Nauch. Tsentr, Akad. Nauk SSSR* **131**, 120-124 (in Russ.). (*Chem. Abstr.* **90**:207442z).
- RAICEVIC, D. & CABRI, L.J. (1976): Mineralogy and concentration of Au- and Pt-bearing placers from the Tulameen River area in British Columbia. *Can. Inst. Mining Metall. Bull.* **69**(770), 111-119.
- RAY, G.E. (1990): The geology and mineralization of the Coquihalla gold belt and Hozameen fault system, southwestern British Columbia. *B.C. Dep. Energy Mines, Petroleum Resources, Bull.* **79**, 1-97.
- SAMUSIKOV, V.P. & PETROVA, N.I. (1983): Correlations between the content of silver, antimony and copper in native gold (deposits of the Yana–Kolyma belt as examples). *In The Typomorphic Features of Ore Minerals from the Endogenic Formations of Yakutia* (B.L. Flerov, ed.). Yakutskii Filial SQ Akad. Nauk SSSR, 39-53 (in Russ.). (*Chem. Abstr.* **101**:114234p).
- STUMPFL, E.F. & CLARK, A.M. (1965): Electron-probe microanalysis of gold platinoid concentrates from southeast Borneo. *Trans. Inst. Mining Metall.* **B 74**, 933-946.
- _____, _____, (1966): Electron-probe microanalysis of gold platinoid concentrates from southeast Borneo. Discussion. *Trans. Inst. Mining Metall.* **B 75**, 306.
- WHITE, J.L., ORR, R.L. & HULTGREN, R. (1957): The thermodynamic properties of silver–gold alloys. *Acta Metall.* **5**, 747-760.
- YAMAUCHI, H., YOSHIMATSU, H., FOROUHI, H. & DE FONTAINE, D. (1981): Phase relations in Cu–Ag–Au ternary alloys. *In Precious Metals 1981. Proc. 4th Int. Metall. Conf.*, 214-249.

Received February 29, 2000, revised manuscript accepted March 31, 2001.